D. J. Mukai
Graduate Student,
Department of Civil Engineering,
University of Washington, FX-10
Seattle, WA 98195

R. Ballarini
Assistant Professor,
Department of Civil Engineering,
Case Western Reserve University,
Cleveland, OH 44106

G. R. Miller
Associate Professor,
Department of Civil Engineering,
University of Washington, FX-10
Seattle, WA 98195
Assoc. Mem. ASME

Analysis of Branched Interface Cracks

A solution is presented for the problem of a finite length crack branching off the interface between two bonded dissimilar isotropic materials. Results are presented in terms of the ratio of the energy release rate of a branched interface crack to the energy release rate of a straight interface crack with the same total length. It is found that this ratio reaches a maximum when the interface crack branches into the softer material. Longer branches tend to have smaller maximum energy release rate ratio angles indicating that all else being equal, a branch crack will tend to turn back parallel to the interface as it grows.

1 Introduction

The interface crack problem was addressed in the late 1950's by Williams (1959). Williams used an eigenfunction expansion technique to solve the interface crack problem and discovered complex singularities and rapid oscillating stresses near the crack tip. Williams also estimated the oscillatory region to be very small.

In the mid 1960's, various workers (England (1965), Erdogan (1965), Rice and Sih (1965)) came up with closed-form solutions to the interface problem. These solutions verified Williams' (1959) finding of complex singularities and rapidly oscillating stresses near the crack tip. England (1965) also pointed out that the complex singularities lead to the physical impossibility of the crack faces interpenetrating near the crack tips. Like Williams (1959), these workers found the region where these phenomena occur was very small.

In the mid-1970's Comninou (1977) put forth an alternate solution that addressed the difficulties at the crack tip. Comninou resolved the problems at the crack tip by solving the interface crack problem assuming there is a small contact zone near the crack tips. This zone was found to be extremely small. While calculations were carried out for a limited range of Dundurs' constants (Dundurs 1969), Comninou's work provides a rational explanation of the oddities occurring near the crack tips.

Lately, the interface crack problem has received renewed attention. Gautensen and Dundurs (1987) have solved the problem formulated by Comninou (1977) using quickly convergent series. Unlike Comninou's (Comninou (1977) results which were carried out for only severe material mismatches, Gautesen and Dundurs obtain results covering all material combinations. Symington (1987) has completed Williams' (Williams 1959) eigenfunction analysis by finding a set of integer eigenvalues left out by Williams. Rice (1988) has proposed that the peculiarities at the crack tip are not too critical. In an argument similar to the concept of small-scale yielding, he asserts that the complex stress intensity factors will be indicative of the general state of the crack tip even if they do not correctly represent the state immediately surrounding the crack tip. Rice also provides a framework to interpret the complex intensity factor in terms of the classical form stress intensity factors K_I and K_{II}. He also includes an interesting discussion of the interaction of the crack length and load phase angle influence. Hutchinson, Mear, and Rice (1987) have looked at a crack completely in one body but very near the interface. Their solution, based on dimensional arguments, energy considerations, and the representation of the crack as a distribution of dislocations, examines criteria for crack growth parallel to the material interface. Park and Earmme (1986) use various integrals to describe the interface crack tip characteristics and include a discussion of the properties of these integrals. Shih and Asaro (1988) have investigated the interface crack with plasticity. They find that the pathological features of the linear elastic analyses are lessened by nonlinear behavior and that the linear elastic solutions are good in regions not immediately around the crack tip. Delale and Erdogan (1988) have looked at the interface crack by modeling the interface as a transition material; they put the crack in a thin third layer between the two half-spaces. They present some results regarding the direction of maximum K_I of the crack. Generally, K_I is larger as the crack tends toward the softer material. He and Hutchinson (1988) have performed an analysis very similar to the present one for the case of a branched semi-infinite crack.

Contributed by the Applied Mechanics Division of THE AMERICAN SOCIETY OF MECHANICAL ENGINEERS for publication in the JOURNAL OF APPLIED MECHANICS.

Discussion on this paper should be addressed to the Technical Editor, Leon M. Keer, The Technological Institute, Northwestern University, Evanston, IL 20208, and will be accepted until two months after final publication of the paper itself in the JOURNAL OF APPLIED MECHANICS. Manuscript received and accepted by the ASME Applied Mechanics Division, Feb. 22, 1989.

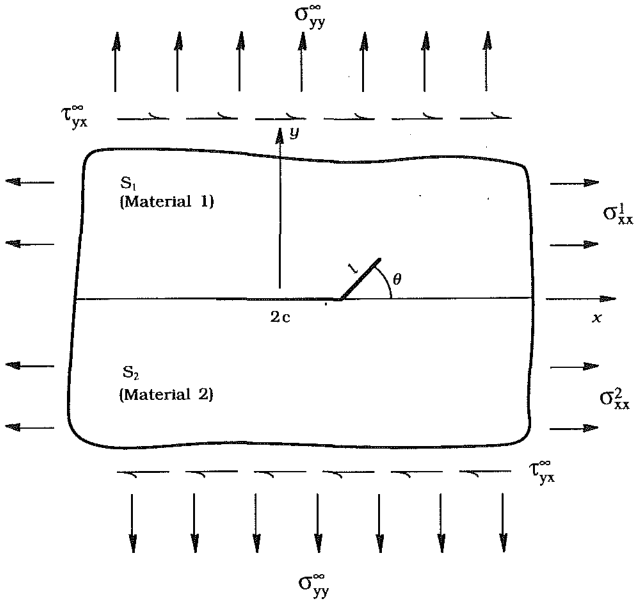

Fig. 1 A branched interface crack

They have presented extensive results on the initial branching angle, couched in terms of strain energy release rates.

In this paper, the branching of a finite length crack is analyzed. For small branch lengths the asymptotic results of He and Hutchinson are reproduced. For longer branch lengths the behavior changes as the global portion of the stress field influences further branch growth. Based on the obtained results, some conjectures are made concerning the fate of branching cracks.

2 Formulation

The problem configuration is depicted in Fig. 1, which shows the main crack, the branch crack, the loading at infinity, and the coordinate system. In the upper half-plane (S_1), the shear modulus is μ_1 and Poisson's ratio is ν_1. In the lower half-plane (S_2), the shear modulus is μ_2 and Poisson's ratio is ν_2. The boundary conditions for this problem require that both the main and branch cracks are traction-free and that at infinity the stresses approach σ_{yy}^{∞} and τ_{yx}^{∞}. Single-valuedness of the displacements at infinity is also required.

Some techniques useful for dealing with interface boundary conditions which are used in the problem formulation are presented first. These results follow directly from the formulation used by Clements (1971) to treat interface cracks in anisotropic materials.

In terms of the Muskhelishvili (1953) potentials, the stresses and displacements in isotropic elastic bodies may be expressed as follows:

$$(\sigma_{yy}-i\tau_{yx})_i=\Phi_i(z)+\overline{\Phi_i(z)}+z\overline{\Phi_i'(z)}+\overline{\Psi_i(z)} \qquad (1)$$

$$(\sigma_{yy}+\sigma_{xx})_i=2[\Phi_i(z)+\overline{\Phi_i(z)}] \qquad (2)$$

$$2\mu_i\left(\frac{\partial u}{\partial x}-i\frac{\partial v}{\partial x}\right)_i=\kappa_i\Phi_i(z)-[\overline{\Phi_i(z)}+z\overline{\Phi_i'(z)}+\overline{\Psi_i(z)}] \qquad (3)$$

in which the subscript $i\,(i=1, 2)$ denotes "in region i", Φ_1, Ψ_1 correspond to the potentials for the upper half-plane and Φ_2, Ψ_2 correspond to the potentials for the lower half-plane. Moreover, z is the complex variable $x+iy$, the prime denotes differentation with respect to z, an overbar denotes conjugation, $\kappa=3-4\nu$ for plane strain, and $\kappa=\dfrac{3-\nu}{1+\nu}$ for plane stress.

For interface problems, it is convenient to introduce additional potentials as follows. Making use of the fact that if $f(z)$ is analytic for z in region R, then $f(z)\equiv\overline{\overline{f(\bar{z})}}$ is analytic for $\bar{z}$ in region R, the following *analytic* jump potentials are constructed:

$$\Omega_s=\begin{cases}\Phi_1(z)-[\overline{\Phi_2}(z)+z\overline{\Phi_2'}(z)+\overline{\Psi_2}(z)] & z\epsilon S_1\\ \Phi_2(z)-[\overline{\Phi_1}(z)+z\overline{\Phi_1'}(z)+\overline{\Psi_1}(z)] & z\epsilon S_2\end{cases} \qquad (4a)$$

$$\Omega_D=\begin{cases}\dfrac{\kappa_1}{2\mu_1}\Phi_1(z)+\dfrac{1}{2\mu_2}[\overline{\Phi_2}(z)+z\overline{\Phi_2'}(z)+\overline{\Psi_2}(z)] & z\epsilon S_1\\ \dfrac{\kappa_2}{2\mu_2}\Phi_2(z)+\dfrac{1}{2\mu_1}[\overline{\Phi_1}(z)+z\overline{\Phi_1'}(z)+\overline{\Psi_1}(z)] & z\epsilon S_2.\end{cases} \qquad (4b)$$

Note that in terms of these jump potentials, the interface conditions can be expressed as:

$$(\sigma_{yy}-i\tau_{yx})_2-(\sigma_{yy}-i\tau_{yx})_1=\Omega_{S2}(x)-\Omega_{S1}(x) \qquad 5(a)$$

$$\left(\frac{\partial u}{\partial x}-i\frac{\partial v}{\partial x}\right)_2-\left(\frac{\partial u}{\partial x}-i\frac{\partial v}{\partial x}\right)_1=\Omega_{D2}(x)-\Omega_{D1}(x). \qquad 5(b)$$

The Ω potentials thus represent the jump in traction (Ω_S) and displacement (Ω_D) across the interface. The inverse relationship between the jump and Muskhelishvili potentials is determined algebraically from equations (4):

$$\Phi_1(z)=Q_1\left[\frac{1}{2\mu_2}\Omega_{S1}(z)+\Omega_{D1}(z)\right] \qquad (6a)$$

$$\Psi_1(z)=Q_2\left[\frac{-\kappa_2}{2\mu_2}\overline{\Omega}_{S2}(z)+\overline{\Omega}_{D2}(z)\right]-\Phi_1(z)-z\Phi_1'(z) \qquad (6b)$$

$$\Phi_2(z)=Q_2\left[\frac{1}{2\mu_1}\Omega_{S2}(z)+\Omega_{D2}(z)\right] \qquad (6c)$$

$$\Psi_2(z)=Q_1\left[\frac{-\kappa_1}{2\mu_1}\overline{\Omega}_{S1}(z)+\overline{\Omega}_{D1}(z)\right]-\Phi_2(z)-z\Phi_2'(z) \qquad (6d)$$

where

$$Q_1=\frac{2\mu_1\mu_2}{\mu_1+\kappa_1\mu_2} \qquad (7a)$$

$$Q_2=\frac{2\mu_1\mu_2}{\mu_2+\kappa_2\mu_1}. \qquad (7b)$$

This formulation allows for straightforward development of the various interaction potentials derived below.

3 Solution

The solution is obtained by a Green's function technique based on distributing dislocation singularities along the branch. The solution for the interaction between an interface crack and a dislocation is found by superposing the solutions for: (1) a dislocation in S_1 near an interface; (2) two perfectly bonded semi-infinite bodies loaded at infinity with σ_{yy} and τ_{yx}; and (3) an interface crack loaded with the negative of the stresses produced by (1) and (2). This solution for a single dislocation interacting with an interface crack (with the appropriate far-field loading) is then modified to model a distribution of dislocations along the branch, and by requiring zero tractions along the branch face a singular integral equation is obtained for the unknown dislocation distribution. The relevant physical quantities can be calculated after numerically solving the integral equation.

Most of the component solutions to be superposed are well-known. Nevertheless, it is convenient to rederive them here using the framework presented in Section 2. This will provide a consistent formulation, as well as a demonstration of the generality of the approach.

Consider first a dislocation near an interface (see Head, 1953; Dundurs and Sendeckyj (1965) located at a point z_0 in the upper half-plane. The continuity of tractions and displacements across the interface in combination with equation (5) implies the following boundary conditions on the jump potentials:

$$\left.\begin{array}{l}\Omega_{S1}^{D}-\Omega_{S2}^{D}=0\\ \Omega_{D1}^{D}-\Omega_{D2}^{D}=0\end{array}\right\}|x|<\infty, y=0. \tag{8}$$

The singular portion of the jump potentials can be obtained directly by transforming the known singular potentials for a dislocation in a homogeneous full-plane into jump potentials. For a full-plane dislocation in region 1 we have:

$$\Phi_{1,\ \text{Singular}}^{D}=\frac{A}{z-z_0} \tag{9(a)}$$

$$\Psi_{1,\ \text{Singular}}^{D}=\frac{\bar{A}}{z-z_0}+A\frac{\bar{z}_0}{(z-z_0)^2} \tag{9(b)}$$

$$\Phi_{2,\ \text{Singular}}^{D}=\Psi_{2,\ \text{Singular}}^{D}=0 \tag{9(c)}$$

in which $A=\mu_1 e^{i\theta}\{[u_r]+i[v_\theta]\}/i\pi(\kappa_1+1)$, with $[u_r]$ and $[v_\theta]$ representing the jumps in the tangential and normal displacements accrued upon circling the dislocation. The corresponding Ω potentials are determined from equation (4):

$$\Omega_{S1,\ \text{Singular}}^{D}=\frac{A}{z-z_0} \tag{10a}$$

$$\Omega_{S2,\ \text{Singular}}^{D}=-\left[\frac{A}{z-\bar{z}_0}+\bar{A}\frac{z_0-\bar{z}_0}{(z-\bar{z}_0)^2}\right] \tag{10b}$$

$$\Omega_{S1,\ \text{Singular}}^{D}=\frac{\kappa_1}{2\mu_1}\frac{A}{z-z_0} \tag{10c}$$

$$\Omega_{S2,\ \text{Singular}}^{D}=\frac{1}{2\mu_1}\left[\frac{A}{z-\bar{z}_0}+\bar{A}\frac{z_0-\bar{z}_0}{(z-\bar{z}_0)^2}\right]. \tag{10d}$$

Obviously, the boundary conditions given by equation (8) are not satisfied. To patch up the interface boundary conditions, potentials of the following form are added, which are analytic in their respective regions:

$$\Omega_{S1,\ \text{Continuation}}^{D}=\Omega_{S2,\ \text{Singular}}^{D};\ z\in S_1 \tag{11a}$$

$$\Omega_{S2,\ \text{Continuation}}^{D}=\Omega_{S1,\ \text{Singular}}^{D};\ z\in S_2 \tag{11b}$$

with similar expressions for the displacement jump potentials. Using equation (6) to invert these to regular potentials gives the additional terms to be added to the singular potentials in equation (9) to give the desired solution (i.e., $\Phi^D=\Phi_{\text{Continuation}}^{D}+\Phi_{\text{Singular}}^{D}$, etc.):

$$\Phi_{1,\ \text{Continuation}}^{D}=A\left[\frac{(\alpha-\beta)}{(1+\beta)(z-\bar{z}_0)}\right]+\bar{A}\left[\frac{(\alpha-\beta)(z_0-\bar{z}_0)}{(1+\beta)(z-\bar{z}_0)^2}\right] \tag{12a}$$

$$\Psi_{1,\ \text{Continuation}}^{D}=\bar{A}\left[\frac{(\alpha+\beta)}{(1-\beta)(z-\bar{z}_0)}\right]-\Phi_{1,\ \text{Continuation}}^{D}-z\Phi_{1,\ \text{Continuation}}^{D\prime} \tag{12b}$$

$$\Phi_{2,\ \text{Continuation}}^{D}=A\left[\frac{1+\alpha}{(1-\beta)(z-z_0)}\right] \tag{12c}$$

$$\Psi_{2,\ \text{Continuation}}^{D}=A\left[\frac{(1+\alpha)(\bar{z}_0-z_0)}{(1+\beta)(z-z_0)^2}\right]+\bar{A}\left[\frac{(1+\alpha)}{(1+\beta)(z-z_0)}\right]-\Phi_{2,\ \text{Continuation}}^{D}-z\Phi_{2,\ \text{Continuation}}^{D\prime} \tag{12d}$$

where α and β are Dundurs' (Dundurs, 1969) constants defined by:

$$\alpha=\frac{\mu_2(\kappa_1+1)-\mu_1(\kappa_2+1)}{\mu_2(\kappa_1+1)+\mu_1(\kappa_2+1)} \tag{13a}$$

$$\beta=\frac{\mu_2(\kappa_1-1)-\mu_1(\kappa_2-1)}{\mu_2(\kappa_1+1)+\mu_1(\kappa_2+1)}. \tag{13b}$$

The constant potentials corresponding to the far-field loading can be derived from the jump potentials by simply starting with constant Ω's, which automatically satisfy the interface conditions, and inverting to determine the corresponding Φ's. The details of this operation are in the Appendix; the results are as follows:

$$\Phi_1^\infty=\frac{\sigma_{yy}^\infty+\sigma_{xx1}^\infty}{4}+i\left[\frac{(\beta-1)\tau_{yx}^\infty}{2}+\frac{1-\alpha}{2}IC_S\right] \tag{14a}$$

$$\Psi_1^\infty=\frac{\sigma_{yy}^\infty-\sigma_{xx1}^\infty}{2}+i\tau_{yx}^\infty \tag{14b}$$

$$\Phi_2^\infty=\frac{\sigma_{yy}^\infty+\sigma_{xx2}^\infty}{4}+i\left[-\frac{(\beta+1)\tau_{yx}^\infty}{2}+\frac{1-\alpha}{2}IC_S\right] \tag{14c}$$

$$\Psi_2^\infty=\frac{\sigma_{yy}^\infty-\sigma_{xx2}^\infty}{2}+i\tau_{yx}^\infty \tag{14d}$$

in which the arbitrary constant IC_S does not affect the stresses and is related to a rigid body rotation. For convenience, it is chosen so the Imag $\{\Phi_{1,\ \text{Far Field}}\}=0$. This gives Imag $\{\Phi_{2,\ \text{Far Field}}\}=\dfrac{\alpha-\beta}{1-\alpha}\tau_{yx}$.

In determining the relations (14), it turns out that the $x-$direction stresses are related:

$$\sigma_{xx2}=\frac{4\beta-2\alpha}{1-\alpha}\sigma_{yy}^\infty+\frac{1+\alpha}{1-\alpha}\sigma_{xx1} \tag{15}$$

This result for σ_{xx2} and σ_{xx1} is typical of interface problems (see, e.g., Dundurs (1969)). Since this analysis will be considering branches which are not strictly parallel to the x-axis, these x-direction stresses are important: They cannot be ignored as in the normal interface crack problem. Since it is generally not possible to have these stresses vanish in both regions simultaneously, some choice must be made for their values. The choice made here is to take $\sigma_{xx2}=-\sigma_{xx1}$, which implies that the net force on a vertical cut is zero. It was verified using a finite element analysis of bonded interface bodies of finite dimensions that there exists a region at the center of the specimens near the interface where the tensile stress parallel to the interface in one body is equal and opposite to the tensile stress parallel to the interface in the other body. Thus, the present choice of x-direction stresses would be appropriate for interface cracks far from free boundaries with no applied x-direction tractions.

It is now necessary to introduce the main crack. The stresses due to the dislocation near an interface and the far-field loading will be removed from the crack faces by the following potentials:

$$\Phi^C=\Phi_{\text{Dislocation}}^{C}+\Phi_{\text{Far Field}}^{C} \tag{16a}$$

$$\Psi^C=\Psi_{\text{Dislocation}}^{C}+\Psi_{\text{Far Field}}^{C} \tag{16b}$$

where $\Phi_{\text{Dislocation}}^{C}$ removes the stresses on the crack face due to the dislocation and $\Phi_{\text{Far Field}}^{C}$ removes the stresses due to the far-field loading.

To obtain these potentials, first consider the interface crack under arbitrary crack face loading (the standard solution has been presented by many investigators e.g., England, 1965; Erdogan, 1965; Rice and Sih, 1965). For a crack on an interface, the interface boundary conditions are:

$$(\sigma_{yy}-i\tau_{yx})_1-(\sigma_{yy}-i\tau_{yx})_2=0 \qquad |x|<\infty,\ y=0 \qquad (17a)$$

$$(u'-iv')_1-(u'-iv')_2=0 \qquad |x|>c \qquad (17b)$$

$$\sigma_{yy}-i\tau_{yx}=f(x) \qquad |x|<c. \qquad (17c)$$

These boundary conditions, in terms of the standard potentials, are somewhat cumbersome. However, as shown by equation (6), in terms of the jump potentials the first boundary condition is simply:

$$\Omega_{S1}(x)-\Omega_{S2}(x)=0 \qquad |x|<\infty. \qquad (18)$$

Using an argument similar to the one in the far-field solution (see the Appendix), since Ω_S is analytic everywhere and bounded, by Liouville's theorem it must be constant. Moreover, for zero stress at infinity, $\Omega_S=0$.

The second boundary condition in terms of the jump potentials is:

$$\Omega_{D1}(x)-\Omega_{D2}(x)=0 \qquad |x|>c. \qquad (19)$$

The third boundary condition in terms of the jump potentials is:

$$Q_1\Omega_{D1}(x^+)+Q_2\Omega_{D2}(x^-)=f(x^+)=f(x) \qquad |x|<c \qquad (20a)$$

$$Q_2\Omega_{D2}(x^-)+Q_1\Omega_{D1}(x^+)=f(x^-)=f(x) \qquad (20b)$$

or

$$\Omega_D^+ + m\Omega_D^- = \frac{1}{Q_1}f(x) \quad ;|x|<c \qquad (21a)$$

$$m=\frac{Q_2}{Q_1}=\frac{1+\beta}{1-\beta}. \qquad (21b)$$

These last two boundary conditions (equations (19) and (21*a*)) define a Hilbert problem, with the well-known solution:

$$\Omega_D(z)=\frac{X(z)}{2\pi i}\int_{-c}^{+c}\frac{1}{Q_1}\frac{f(x)}{X^+(x)(x-z)}\,dx+X(z)P(z) \qquad (22)$$

in which

$$X(z)=(z-c)^{\gamma-1}(z+c)^{-\gamma}$$

$$\gamma=\frac{1}{2}-\frac{i}{2\pi}\log m=\frac{1}{2}+i\epsilon$$

$$\epsilon=\frac{1}{2\pi}\log\frac{1}{m}$$

and $P(z)$ is a polynomial determined by far-field behavior. After Ω_D is obtained, the jump potentials can be inverted back to standard potentials using equation (6).

To remove the stresses on the crack caused by the dislocation solution, the integration in equation (22) is carried out with $f(x)$ equal to the opposite of the tractions due to a dislocation near the interface. These tractions are obtained by substituting equations (9) and (12) into equation (1):

$$\sigma_{yy}-i\tau_{yx}=A\left[\frac{1+\alpha}{1-\beta}\left(\frac{1}{x-z_0}\right)+\frac{1+\alpha}{1+\beta}\left(\frac{1}{x-\overline{z_0}}\right)\right]$$

$$+\overline{A}\left[\frac{1+\alpha}{1+\beta}\frac{(z_0-\overline{z_0})}{(x-\overline{z_0})^2}\right]. \qquad (23)$$

The resulting jump potentials are

$$\Omega^C_{S,\ \text{Dislocation}}=0 \qquad (24a)$$

$$\Omega^C_{D,\ \text{Dislocation}}=\frac{-2A}{1+m}\frac{1}{Q_1}\left[\frac{1+\alpha}{1-\beta}F(z,z_0)+\frac{1+\alpha}{1+\beta}F(z,\overline{z_0})\right]$$

$$-\frac{2\overline{A}}{1+m}\frac{1}{Q_1}(z_0-\overline{z_0})\left[\frac{1+\alpha}{1+\beta}G(z,\overline{z_0})\right]$$

$$+X(z)P(z) \qquad (24b)$$

in which

$$F(z,a)=\frac{1}{2}\frac{1}{(z-a)}\left[1-\frac{X(z)}{X(a)}\right] \qquad (25a)$$

$$G(z,a)=\frac{\partial F(z,a)}{\partial a}. \qquad (25b)$$

Inverting these to standard potentials gives:

$$\Phi^C_{1,\ \text{Dislocation}}=-\frac{2A}{1+m}\left[\frac{1+\alpha}{1-\beta}F(z,z_0)\right.$$

$$\left.+\frac{1+\alpha}{1+\beta}F(z,\overline{z_0})\right]$$

$$-\frac{2\overline{A}}{1+m}(z_0-\overline{z_0})\left[\frac{1+\alpha}{1+\beta}G(z,\overline{z_0})\right] \qquad (26a)$$

$$\Psi^C_{1,\ \text{Dislocation}}=-\frac{2mA}{1+m}(\overline{z_0}-z_0)\left[\frac{1+\alpha}{1+\beta}\overline{G(\overline{z},\overline{z_0})}\right]$$

$$-\frac{2m\overline{A}}{1+m}\left[\frac{1+\alpha}{1-\beta}\overline{F(\overline{z},z_0)}+\frac{1+\alpha}{1+\beta}\overline{F(\overline{z},\overline{z_0})}\right]$$

$$-\Phi^C_{1,\ \text{Dislocation}}-z\Phi^{C\prime}_{1,\ \text{Dislocation}} \qquad (26b)$$

$$\Phi^C_{2,\ \text{Dislocation}}=-\frac{2mA}{1+m}\left[\frac{1+\alpha}{1-\beta}F(z,z_0)+\frac{1+\alpha}{1+\beta}F(z,\overline{z_0})\right]$$

$$-\frac{2m\overline{A}}{1+m}(z_0-\overline{z_0})\left[\frac{1+\alpha}{1+\beta}G(z,\overline{z_0})\right] \qquad (26c)$$

$$\Psi^C_{2,\ \text{Dislocation}}=--\frac{2A}{1+m}(\overline{z_0}-z_0)\left[\frac{1+\alpha}{1+\beta}\overline{G(\overline{z},\overline{z_0})}\right]$$

$$-\frac{2\overline{A}}{1+m}\left[\frac{1+\alpha}{1-\beta}\overline{F(\overline{z},z_0)}+\frac{1+\alpha}{1+\beta}\overline{F(\overline{z},\overline{z_0})}\right]$$

$$-\Phi^C_{2,\ \text{Dislocation}}-z\Phi^{C\prime}_{2,\ \text{Dislocation}}. \qquad (26d)$$

Each of the potentials in equation (26) contains an $X(z)P(z)$ term following inversion. However, requiring that the stresses vanish at infinity and requiring that there be no net displacement at infinity (no net $1/z$ term) leads to all the $P(z)$'s being zero.

Removal of the constant far-field tractions is simply the standard interface problem. After performing the necessary integrals in equation (22), the Ω potentials are:

$$\Omega^C_{S,\ \text{Far Field}}=0 \qquad (27a)$$

$$\Omega^C_{D,\ \text{Far Field}}=-\frac{\sigma^\infty_{yy}-i\tau^\infty_{yx}}{(1+m)Q_1}+\frac{\sigma^\infty_{yy}-i\tau^\infty_{yx}}{(1+m)Q_1}[z+(2\gamma-1)c]X(z)$$

$$+P(z)X(z) \qquad (27b)$$

Again, $P(z)$ is determined by far-field behavior and turns out to be zero. Inverting to standard potentials gives the following result, which is of course identical to the previous solutions mentioned earlier:

$$\Phi^C_{1,\text{ Far Field}} = \frac{\sigma^\infty_{yy} - i\tau^\infty_{yx}}{(1+m)} [X(z)\{z-(1-2\gamma)c\}-1] \tag{28a}$$

$$\Psi^C_{1,\text{ Far Field}} = \frac{m(\sigma^\infty_{yy} + i\tau^\infty_{yx})}{(1+m)} [\bar{X}(Z)\{z - (1-2\bar{\gamma})c\}-1] - \Phi_1 - z\Phi_1' \tag{28b}$$

$$\Phi^C_{2,\text{ Far Field}} = \frac{m(\sigma^\infty_{yy} - i\tau^\infty_{yx})}{(1+m)} [X(z)\{z-(1-2\gamma)c\}-1] \tag{28c}$$

$$\Psi^C_{2,\text{ Far Field}} = \frac{\sigma^\infty_{yy} - i\tau^\infty_{yx}}{(1+m)} [\bar{X}(z)\{z-(1-2\bar{\gamma})c\}-1] - \Phi_2 - z\Phi_2'. \tag{28d}$$

The final potentials that give the solution to the interaction between a discrete dislocation and an interface crack subjected to uniform far-field stresses are:

$$\Phi_1 = \Phi^D_1 + \Phi^\infty_1 + \Phi^C_1 \tag{29a}$$

$$\Psi_1 = \Psi^D_1 + \Psi^\infty_1 + \Psi^C_1 \tag{29b}$$

where the Dislocation (D) potentials, the infinity (∞) potentials and the Crack (C) potentials are all defined above. For the no interface case ($\alpha=\beta=0$) the present solution reduces analytically to Lo's (Lo, 1978) solution.

Replacing the discrete dislocation with a continuous distribution of dislocations enables the modeling of the crack branch. Requiring the traction to be zero on the branch leads to an integral equation in terms of the unknown dislocation density. After nondimensionalizing and separating the kernel into singular and regular parts, the following Cauchy-type integral equation is arrived at:

$$\int_{-1}^{1} \frac{D(t)}{t-s}\,dt + \frac{l/c}{2}\int_{-1}^{1}[\tilde{K}_1(s,t)D(t) + \tilde{K}_2(s,t)\bar{D}(t)]dt = -f(s) \tag{30}$$

in which $D(t) = \mu_1 e^{i\theta}\partial/\partial t\{[u_r]+i[v_\theta]\}/i\pi(\kappa_1+1)$ along the line $z_0 = 1 + te^{i\theta}$, $[u_r]$ and $[v_\theta]$ are the jumps in the tangential and normal displacements across the dislocation line, $\tilde{K}_1$ and $\tilde{K}_2$ are the kernels resulting from the potentials derived earlier, and $f(s)$ is the known traction along the branch line $z=1+se^{i\theta}$ due to the main crack loaded at infinity.

This equation is solved numerically using piecewise continuous polynomials in the manner of Gerasoulis (1982). Once the dislocation densities have been determined numerically, the stress intensity factors are obtained directly from the dislocation density at the tip of the branch crack in the normal fashion (e.g., Bryant, Miller, and Keer, 1984). In applying the numerical scheme, the integration point at the base of the branch crack is eliminated. Ignoring the integration point at the "knee" of the branched crack is an approximate method of incorporating the fact that the singularity at this end of the crack is less than one half. In their asymptotic analysis, He and Hutchinson (1988) investigated the effect of neglecting this integration point as opposed to including the actual singularity explicitly and found the effect to be minimal. Although it does not necessarily follow that the minimal effect of ignoring the integration point in the asymptotic problem holds true for the finite length crack problem, for those cases where one would expect the most problems (short branch lengths) the calculated results match those of He and Hutchinson quite well. Thus, despite the approximate nature of the handling of the junction of the main crack with the branch, the numerical solution provides accurate results for the branching problem.

4 Numerical Results and Conclusions

Although shear loading at infinity is included in the formulation of the problem, it is not included in the numerical results since the resulting large contact zones at the crack tips change the requirements of the solution procedure quite drastically. For this reason, the integral equation (30) was solved numerically for pure tensile load at infinity only (σ^∞_{yy}). Although results are presented as follows for a small set of material parameters, calculations were actually carried out over the entire α,β plane, with some not unexpected numerical difficulties arising in the vicinity of extreme material mismatches. The presented results are representative of these more wide-ranging calculations.

For purposes of linking up to the asymptotic results of He and Hutchinson (1988), the parameter of interest is taken as $\mathcal{G}/\mathcal{G}_0$; the ratio of the energy release rate at the tip of the branch to the energy release rate at an equivalent unbranched interface crack. For this analysis, $\mathcal{G}$ corresponds to the strain energy release rate of a branch crack tip in material 1 and $\mathcal{G}_0$ corresponds to the strain energy release rate at the tip of an interface crack of total length $2c' = 2c + l$. The expressions for $\mathcal{G}$, $\mathcal{G}_0$, and $\mathcal{G}/\mathcal{G}_0$ are:

$$\mathcal{G} = \left[\frac{1-\nu_1}{2\mu_1}\right](K_I^2 + K_{II}^2) \tag{31a}$$

$$\mathcal{G}_0 = \left[\frac{1-\nu_1}{\mu_1} + \frac{1-\nu_2}{\mu_2}\right]\frac{(\sigma_{yy}^2 + \sigma_{yx}^2)(1+4\epsilon^2)\pi c'}{4\cosh^2(\pi\epsilon)} \tag{31b}$$

$$\frac{\mathcal{G}}{\mathcal{G}_0} = (1+\alpha)\frac{\cosh^2\pi\epsilon}{(1+4\epsilon^2)(\sigma_{yy}^{\infty 2} + \tau_{yx}^{\infty 2})}\left[\left(\frac{K_I}{\sqrt{\pi c'}}\right)^2 + \left(\frac{K_{II}}{\sqrt{\pi c'}}\right)^2\right]. \tag{31c}$$

As the length of the branch becomes very small relative to the main crack, it is expected that the present results should in some sense approach those of the semi-infinite crack. However, as explained below, the present results can be directly compared to He and Hutchinson's (1988) asymptotic results only for $\beta=0$. Figure 2 shows the dependence of the strain energy release, rate, $\mathcal{G}/\mathcal{G}_0$ on the branch angle, θ for $\alpha=0.5$, $\beta=0$, and $1/c = 0.0001$. The $\mathcal{G}/\mathcal{G}_0$ results in Fig. 2 indeed agree well with those of He and Hutchinson (1988), as expected.

For $\beta \neq 0$, there are some interesting problems regarding the loading parameter. As shown by Rice (1988), the far-field loading and crack length are coupled in the expression for the complex intensity factor $K = K_1 + iK_2 = (k_1 + ik_2)\sqrt{\pi}\cos(\pi\epsilon)$, where $k_1 + ik_2$ is the complex intensity factor of Sih and Rice (1964). Since He and Hutchinson (1988) used $\gamma = \tan^{-1}K_2/K_1$

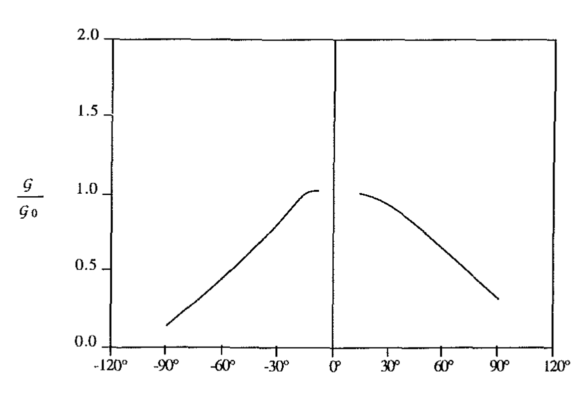

Fig. 2 Strain energy release rate ratio, $\mathcal{G}/\mathcal{G}_0$, versus extension angle, θ, for $l/c = 0.001$, $\alpha = 0.5$, $\beta = 0$ (e.g., $\Gamma = 3$, $\nu_1 = \nu_2 = 0.5$)

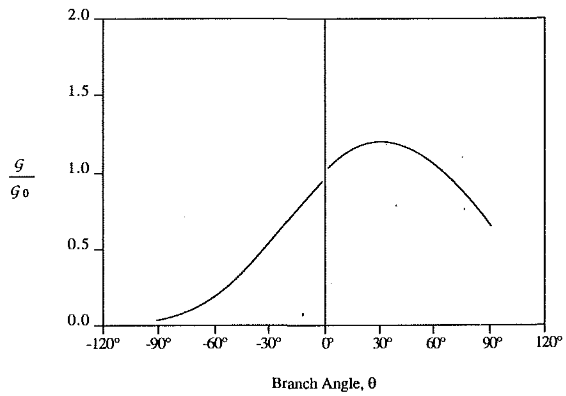

Fig. 3 Strain energy release rate ratio, $\mathcal{G}/\mathcal{G}_0$, versus extension angle, θ, for $l/c = 0.001$, $\nu_1 = \nu_2 = 0.3$, $\Gamma = 3$ ($\alpha = 0.5$, $\beta = 0.14286$)

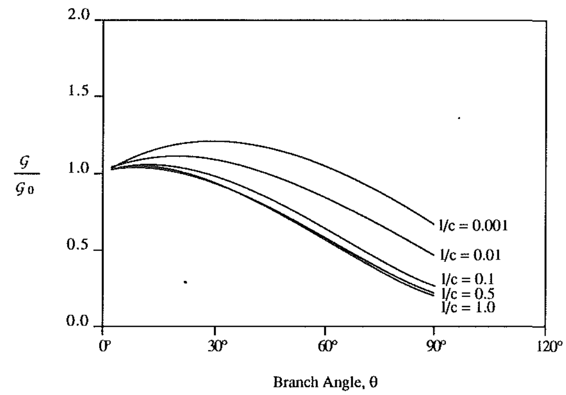

Fig. 5 Strain energy release rate ratio, $\mathcal{G}/\mathcal{G}_0$, versus extension angle, θ, for $\nu_1 = \nu_2 = 0.3$, $\Gamma = 3$, $l/c = 0.001$, 0.01, 0.1, 0.5, 1 ($\alpha = 0.5$, $\beta = 0.14286$)

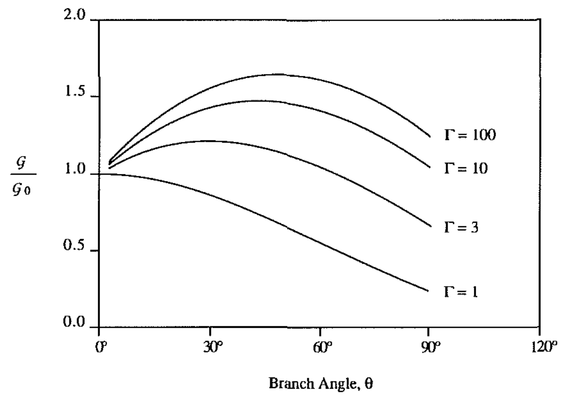

Fig. 4 Strain energy release rate ratio, $\mathcal{G}/\mathcal{G}_0$, versus extension angle, θ, for $l/c = 0.001$, $\nu_1 = \nu_2 = 0.3$, $\Gamma = 1$, 3, 10, 100 ($\alpha = 0$, 0.5, 0.81818, 0.98020; $\beta = 0$, 0.14286, 0.23377, 0.28006)

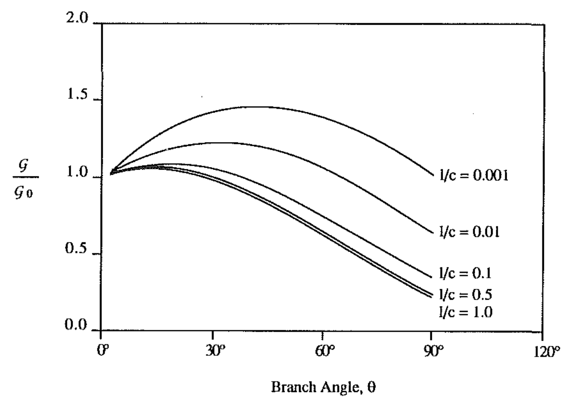

Fig. 6 Strain energy release rate ratio, $\mathcal{G}/\mathcal{G}_0$, versus extension angle, θ, for $\nu_1 = \nu_2 = 0.3$, $\Gamma = 10$, $l/c = 0.001$, 0.01, 0.1, 0.5, 1 ($\alpha = 0.81818$, $\beta = 0.23377$)

as their loading factor, it is not possible to match their loading parameters uniquely for $\beta \neq 0$. Specifically, the loading parameter used here, $\Psi = \tan^{-1}{}^{\infty}_{yx}/\sigma^{\infty}_{yy}$, is related to He and Hutchinson's parameter, γ, by:

$$\Psi = \gamma + \tan^{-1} 2\epsilon - \epsilon \log 2c. \tag{32}$$

In the present analysis, the salient length parameter is the ratio of the branch crack length to the main crack length, l/c, and the absolute value of c is arbitrary. Since the value of c is arbitrary Ψ and γ cannot be related in a definitive manner. Equation (32) shows that for $\beta = 0$, ϵ will be 0 and Ψ is equivalent to γ, and thus the results in Fig. 2 can be directly compared to He and Hutchinson's. Conversely for $\beta \neq 0$, $\Psi \neq \gamma$, the two loading parameters are different. As noted by Rice (1988), ϵ is usually very small. However, because of the $\epsilon \log 2c$ term in equation (32), this does not ensure that $\Psi \cong \gamma$. If $\epsilon \log 2c << 1$, then $\Psi \cong \gamma$.

Figure 3 shows that for the case of the crack growing into the softer material, the maximum $\mathcal{G}/\mathcal{G}_0$, $\mathcal{G}/\mathcal{G}_{0\max}$, occurs at an angle somewhat off the interface and in the softer material ($\theta > 0$). Although it is not shown by these figures, the angle at which K_I is maximized in the softer material corresponds to a nearly zero value for K_{II}. These results are typical for different l/c and $\Gamma s(\Gamma = \mu_2/\mu_1)$, and are consistent with the observations of He and Hutchinson concerning the tendency of branching to occur in the softer material provided the material toughnesses are comparable. Subsequent results are presented for θ in the soft material only.

Figure 4 shows $\mathcal{G}/\mathcal{G}_0$ versus θ for various Γ and $l/c = 0.001$. Notice that as Γ increases, so does $\mathcal{G}/\mathcal{G}_{0\max}$. The angle that maximizes $\mathcal{G}/\mathcal{G}_0$, $\theta_{\max}$, also increases as Γ increases. Again, both these trends agree with He and Hutchinson's (1988) results for $\gamma \neq 0$, although for the reasons given above, direct comparison is no longer possible. It should be noted that the in-plane stresses, σ_{xx}, are increased also by increasing material mismatch, although these stresses appear to have only secondary influence on the branch behavior.

Figures 5 and 6 show the influence of finite main crack size by considering $\mathcal{G}/\mathcal{G}_0$ versus θ for various l/c values. In both Fig. 5 and 6, l/c increases, $\mathcal{G}/\mathcal{G}_{0\max}$ decreases towards a value of unity, while the branch angle corresponding to maximum energy release rate decreases. (Note, however, that in calculating $\mathcal{G}/\mathcal{G}_0$, $\mathcal{G}_0$ is adjusted to be the strain energy release rate for a crack of length $2c + l$. Thus, $\mathcal{G}_{\max}$ itself is not necessarily decreasing with increasing branch length, since $\mathcal{G}_0$ is increasing with l. In fact, $\mathcal{G}_{\max}$ reaches a minimum and then starts to increase again as l/c is increased). Using $\mathcal{G}/\mathcal{G}_{0\max}$ as a crack growth criterion, the decreasing $\theta_{\max}$ with increasing branch length can be taken as an indication that the branch would tend to turn back parallel to the interface as it grows (this rough method for predicting crack trajectories does not always work; see Rubinstein, 1989). Given the further result that the maximum energy release rate at the branch tip approaches that of the interface crack itself as the branch grows, then together this would imply that in a limited sense branching is irrelevant, since the driving force would be similar whether branching occurs or not. The critical issue, however, remains the relative toughnesses of the materials involved.

The primary conclusions to be drawn from the present analysis are that branching from an interface is a viable mode of crack growth, and that such branching is likely to occur initially at an angle somewhere between 10 deg and 47 deg in the softer of the two materials, provided the material toughnesses are similar. As the branch extends its growth characteristics will be altered, resulting in a tendency to return to a path parallel to the interface, with a driving force similar to that of an unbranched crack.

Acknowledgments

This material is based upon work supported by the National Science Foundation under Grant No. MSM-8657628, and by NASA-Lewis under Grant No. NAG3-856.

References

Bryant, M. D., Miller, G. R., and Keer, L. M., 1984, "Line Contact Between A Rigid Indenter and a Damaged Elastic Body," ASME JOURNAL OF APPLIED MECHANICS, Vol. 37, pp. 467–478.

Clements, D. L., 1971, "A Crack Between Dissimilar Anisotropic Media," *International Journal of Engineering Science*, Vol. 9, pp. 257–265.

Comninou, M., 1977, "The Interface Crack," ASME JOURNAL OF APPLIED MECHANICS, Vol. 44, pp. 631–636.

Delale, F., and Erdogan, F., 1988, "On the Mechanical Modeling of the Interfacial Region in Bonded Half-Planes," ASME JOURNAL OF APPLIED MECHANICS, Vol. 55, pp. 317–324.

Dundurs, J., 1969, Discussion of "Edge-Bonded Dissimilar Orthogonal Elastic Wedges Under Normal and Shear Loading," ASME JOURNAL OF APPLIED MECHANICS, Vol. 36, pp. 650–652.

Dundurs, J., and Sendeckyj, G. P., "Behavior of an Edge Dislocation near a Bimaterial Interface," *Journal of Applied Physics*, Vol. 36, pp. 3353–3354.

England, A. H., 1965, "A Crack Between Dissimilar Media," ASME JOURNAL OF APPLIED MECHANICS, Vol. 32, pp. 400–402.

Erdogan, F., 1965, "Stress Distribution in Bonded Dissimilar Materials With Cracks," ASME JOURNAL OF APPLIED MECHANICS, Vol. 32, pp. 403–410.

Gautesen, A. K., and Dundurs, John, 1987, "The Interface Crack in a Tension Field," ASME JOURNAL OF APPLIED MECHANICS, Vol. 54, pp. 93–98.

Gerasoulis, A., 1982, "The Use of Piecewise Quadratic Polynomials for the Solution of Singular Integral Equations of Cauchy Type," *Computational Mathematics with Applications*, Vol. 8, pp. 15–22.

He, M. Y., and Hutchinson, J. W., 1988, "Kinking of a Crack Out of an Interface," *Harvard Report Mech-13*, Cambridge, Mass.

Head, A. K., 1953, "Edge Dislocations in Inhomogeneous Media," *Proceedings of the Physical Society, London*, Vol. B66, p. 793–801.

Hutchinson, J. W., Mear, M., and Rice, J. R., 1987, "Crack Paralleling an Interface Between Dissimilar Materials," ASME JOURNAL OF APPLIED MECHANICS, Vol. 54, pp. 828–832.

Lo, K. K., 1978, "Analysis of Branched Cracks," ASME JOURNAL OF APPLIED MECHANICS, Vol. 45, pp. 797–802.

Muskhelishvili, N. I., 1953, *Singular Integral Equations*, Noordhoff, Groningen.

Park, J. H., Earmme, Y. Y., 1986, "Application of Conservation Integrals to Interfacial Crack Problems," *Mech. Mater.*, Vol. 5, pp. 261–276.

Rice, J. R., 1988, "Elastic Fracture Mechanics Concepts for Interfacial Cracks," ASME JOURNAL OF APPLIED MECHANICS, Vol. 55, pp. 98–103.

Rice, J. R., and Sih, G. C., 1965, "Plane Problems of Cracks in Dissimilar Media," ASME JOURNAL OF APPLIED MECHANICS, Vol. 32, pp. 418–423.

Rubinstein, A. A., 1989, "Analysis of a Crack Path in a Heterogeneous Stress Field," *Proceedings of the First Pan American Conference of Applied Mechanics*, Rio de Janeiro, Brazil, Jan. 3–6, 1989.

Shih, C. F., and Asaro, R. J., 1988, "Elastic-Plastic Analysis of Cracks on Bimaterial Interfaces: Part 1—Small Scale Yielding," ASME JOURNAL OF APPLIED MECHANICS, Vol. 55, pp. 299–316.

Sih, G. C., and Rice, J. R., 1964, "The Bending of Plates of Dissimilar Materials With Cracks," ASME JOURNAL OF APPLIED MECHANICS, Vol. 31, pp. 477–482.

Symington, M. F., 1987, "Eigenvalues for Interface Cracks in Linear Elasticity," ASME JOURNAL OF APPLIED MECHANICS, Vol. 54, pp. 973–974.

Williams, M. L., 1959, "Stresses Around a Fault or Crack in Dissimilar Media," *Bulletin of the Seismological Society of America*, Vol. 49, pp. 199–204.

APPENDIX

The boundary conditions for the interface body (no crack) under remote stress are:

$$\left.\begin{array}{l}\Omega_{S1}-\Omega_{S2}=0\\ \Omega_{D1}-\Omega_{D2}=0\end{array}\right\}|x|<\infty, y=0. \tag{A1}$$

As pointed out earlier, Ω_{S1}, Ω_{D1} and Ω_{S2}, Ω_{S2} are analytic in their respective regions. Moreover, since these two potentials are equal along the region boundary (as given by the above boundary condition), it can be concluded that Ω_S and Ω_D are analytic everywhere. By Liouville's theorem, since Ω_S and Ω_D are analytic everywhere and bounded, they must be constant. Thus, set:

$$\Omega_S^\infty = C_S = RC_S + iIC_S \tag{A2a}$$

$$\Omega_D^\infty = C_D = RC_D + iIC_D \tag{A2b}$$

in which RC_S, IC_S, RC_D, and IC_D are real constants.

Inverting relations equation (A2) to Muskhelishvili (1953) potentials gives:

$$\Phi_1^\infty = Q_1\left[\frac{1}{2\mu_2}C_S + C_D\right] \tag{A3}$$

$$\Psi_1^\infty = Q_2\left[\frac{-\kappa_2}{2\mu_2}\overline{C_S} + \overline{C_D}\right] - Q_1\left[\frac{1}{2\mu_2}C_S + C_D\right] \tag{A3b}$$

$$\Phi_2^\infty = Q_2\left[\frac{1}{2\mu_1}C_S + C_D\right] \tag{A3c}$$

$$\Psi_2^\infty = Q_1\left[\frac{-\kappa_1}{2\mu_1}\overline{C_S} + \overline{C_D}\right] - Q_2\left[\frac{1}{2\mu_1}C_S + C_D\right]. \tag{A3d}$$

The two complex constants C_S and C_D are determined from the conditions at infinity:

$$\sigma_{yy}^\infty - i\tau_{yx}^\infty = \Phi_i^\infty + \overline{\Phi_i^\infty} + \overline{\Psi_i^\infty} \tag{A4a}$$

$$\sigma_{yy}^\infty - \sigma_{xx1}^\infty = 2(\Phi_1^\infty + \overline{\Phi_1^\infty}) \tag{A4b}$$

$$\sigma_{yy}^\infty - \sigma_{xx2}^\infty = 2(\Phi_2^\infty + \overline{\Phi_2^\infty}) \tag{A4c}$$

Inverting these leads to the expressions in equation (14).